

A MICRO-DAMAGE INVESTIGATION ON A LOW-ALLOY STEEL TESTED USING A 7.62-mm AP PROJECTILE

RAZISKAVA MIKROPOŠKODB MALOLEGIRANEGA JEKLA PO PREIZKUSU S KROGLO AP 7,62 mm

Teyfik Demir¹, Mustafa Übeyli²

¹TOBB University of Economics and Technology, Engineering Faculty, Mechanical Engineering, 06560 Ankara - TÜRKİYE

²Osmaniye Korkut Ata University, Engineering Faculty, Mechanical Engineering, 80000 Osmaniye - TÜRKİYE
mubeyli@gmail.com

Prejem rokopisa – received: 2011-01-21; sprejem za objavo – accepted for publication: 2011-02-23

Low-alloy steels have been widely used as an armor material in defense systems due to their superior mechanical and weldability properties. In this study, microdamage formation in an AISI 4140 steel, which was hit by 7.62-mm armor-piercing (AP) projectile, was investigated. Analyses of the microstructure and microhardness after ballistic testing were performed to correlate the microstructure-property relationship. Two different types of adiabatic shear band (ASB) were observed in the tested samples. The experimental results indicated that the type and hardness of the bands were strongly related to the hardness and ballistic performance of the steel specimens.

Keywords: high-strength steel, adiabatic shear band, armor.

Malolegirana jekla se uporabljajo za obrambne sisteme predvsem zaradi njihovih boljših lastnosti in varivosti. V tem delu je raziskan nastanek poškodbe v jeklu AISI 4140 po udarcu prebojne krogle 7,62 mm v oklep. Mikrostruktura in mikrotvrdota sta po balističnem preizkusu korelirana z odnosom mikrostruktura-lastnosti. V preizkusnih vzorcih sta opaženi dve vrsti adiabatских strižnih pasov (ASB). Rezultati so pokazali, da sta vrsta in trdota pasov zelo povezani s trdoto in balističnimi lastnostmi vzorcev jekla.

Ključne besede: visokotrdna jekla, adiabatски strižni pasovi, oklep

1 INTRODUCTION

Microstructural changes, i.e., phase transformations, distortion of grains, elongation of grains, grain refinement, are observed in metallic materials that are exposed to high strain rates and very large strains. With these changes, bands that are different from the original matrix in nature or alignment may form. These bands are termed adiabatic shear bands and they occur in a number of processes, such as dynamic impact, metal forming, ballistic testing, machining and high-strain-rate deformation. The adiabatic shear band phenomenon was first discovered by Zener and Hollomon¹. However, studies on the adiabatic shear band formation accelerated after the year 1970. The thermomechanical instability caused by the presence of local inhomogeneity, inducing local deformation and heating, results in the formation of shear bands². Adiabatic shearing is a special case where the heat generated in the localized bands cannot be transferred easily to the surrounding material due to the strain rate and thermal properties of the material². However, in a real situation some of the heat loss to the surrounding material always occurs. The reason for using the adiabatic term is to indicate that a large part of the heat is retained in the band². This leads to a local temperature increase which may cause a microstructure change in the material³. Adiabatic shearing can lead to a catastrophic failure in materials under high strain rate

deformation^{4,5}. There are two general classifications of the ASBs: deformed and transformed². In the deformed ASBs, there is no change in the microstructure of the materials, but the grains or structure are highly distorted. On the other hand, in the transformed bands, a crystallographic phase change takes place.

Derep⁶ investigated the microstructure transformation induced by the adiabatic shearing in an armor steel tested using a hollow charge. It was observed that a fine-grained, equiaxed structure of delta ferrite consisting of very narrow martensite laths formed in the center of ASBs. In another study, Wittman et al.⁷ investigated the adiabatic shear-band formation in AISI 4340 steel. Also, an investigation of the adiabatic shear band formation in different steels (AISI 1018, AISI 4340 and HY-100) was performed after applying torsion loads at high strain rates⁸. It was mentioned that the shear bands were produced by the dynamic torsional deformation in all cases and they were of the deformed type for the steel AISI 1018, whereas those were transformed for the steel AISI 4340. In addition, Bassim⁹ studied ASB formation in the AISI 4340 steel during high strain rate deformation using a torsional Split Hopkinson Bar System. It was also reported that ASBs initiated at local defects and inhomogeneities. In addition, the specimen geometry and dimensions were found to be contributing factors to the development of ASBs. Furthermore, Duan et al.¹⁰ examined the forma-

tion of adiabatic shear bands in two different grades of steel (medium carbon steel and 30CrMnMo) subjected to the impact of tungsten projectiles. They reported that three kinds of ASBs formed in the 30CrMnMo, while the medium carbon steel did not easily produce ASBs. Moreover, Hu et al.¹¹ investigated the ASB formation in various steels (4130, AISI 1045, modified rolled homogeneous armor steel and AerMet 100) tested by 44 grain-fragment simulating projectiles. It was shown that transformed bands were found in the steels, 4130, modified rolled homogeneous armor steel and AerMet 100, while deformed bands were found in the AISI 1045. Recently, the effect of heat treatment on the ASBs in AISI 4340 steel tested with the Split Hopkinson Pressure Bar was studied¹². It was concluded that heat treatment did not cause any significant effect on the microstructure and hardness of ASBs. In a more recent work, Lins et al.¹³ made a microstructural characterization of the ASBs in an interstitial-free steel deformed at high strain rates ($>2.8 \cdot 10^4 \text{ s}^{-1}$) in a Split Hopkinson Pressure Bar. They found that the deformation twins occurred throughout the microstructure. Recently, a microstructural study on the AISI 4340 and DIN 100Cr6 steels, tested with a 7.62-mm AP projectile, was carried out¹⁴. It was stated that the impact of the AP projectile resulted in the formation of ASBs in all the samples having different hardness levels¹⁴. In addition to the studies conducted on steels, shear band formation in copper¹⁵⁻¹⁷, aluminum^{18,19} and refractory metals²⁰⁻²³ was also examined.

The ballistic behavior of the high-strength, low-alloy steel AISI 4140 with respect to its hardness and areal density was determined against a 7.62-mm armor-piercing (AP) projectile in our previous work²⁴. In this study, a micro-damage analysis in this type of steel after the ballistic testing with the 7.62-mm AP projectile was made.

2 EXPERIMENTAL PROCEDURE

The AISI 4140 steel is a high-strength, low-alloy steel that can be strengthened significantly by applying a martensite formation heat treatment. This steel is used mainly in the automotive industry and for structural applications. The AISI 4140 steel used in this work had 0.40 % C, 1.0 % Cr, 0.2 % Mo, 0.75 % Mn and 0.2 % Si (mass fractions, $w/\%$). Experimental studies were based mainly on two lines: a microstructural examination and a microhardness measurement of the ASBs formed in AISI 4140 steel that was subjected to the impact of a 7.62-mm AP projectile²⁴. This type of projectile is widely used in NATO armies. Its specification can be found in ref.²⁴. The thicknesses of the steel samples utilized in this work were 7.2 mm, 9 mm, 10.8 mm, 12.7 and 14.4 mm. Furthermore, three hardness levels (38 HRC, 50 HRC and 60 HRC) were considered for each thickness of the steel sample for the comparison with the previous study¹⁴. In coding of the steel specimens, the letters A, B and C were used to indicate the hardness levels of 38 HRC, 50 HRC and 60 HRC, respectively. In addition, the

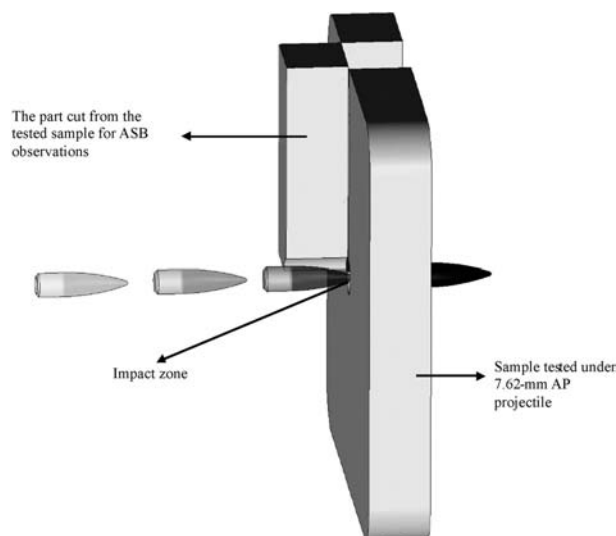


Figure 1: Location of samples for ASB investigation
Slika 1: Mesto odzema vzorcev za preiskave ASB

numbers, 1, 2, 3, 4 and 5 following these letters were utilized to refer to the steel thickness of 7.2 mm, 9 mm, 10.8 mm, 12.7 and 14.4 mm, respectively.

The microstructural changes in the specimens were firstly determined using an optical microscope to see the type and distribution of the ASBs in the material. For this purpose, the AISI 4140 steel specimens were etched using 5 % nital solution to see both the phase(s) and the adiabatic shear bands clearly. Next, the microstructures of the samples were investigated at the impact surfaces through the thickness of the steel and parallel to the projectile motion (**Figure 1**). Secondly, an analysis using a scanning electron microscope (SEM) was carried out to resolve the microstructure of the white ASBs more clearly. Moreover, a representative chemical content of the precipitate was determined by energy-dispersive X-ray (EDX) analysis. Finally, the microhardness measurements were also made to determine the hardness of the different types of adiabatic shear bands formed upon impact.

3 EXPERIMENTAL RESULTS AND DISCUSSION

Typical microstructures of the sample before testing are represented in **Figure 2**. Due to the applied heat treatment, all the samples had a tempered martensite phase containing ferrite with very small iron-carbide islands. This type of phase provides the best combination of strength and toughness for a low-alloy steel. For this reason, this type of microstructure is frequently chosen to be used in high-strength applications.

The kinetic energy of the projectile was able to generate ASBs in the AISI 4140 steel. Its velocity was measured to be $(782 \pm 5.4) \text{ m/s}$ ²⁴. The most important factor in ballistic studies is the velocity of the impact. Damage types change significantly with the impact velocity. The velocities between 700 m/s and 3000 m/s are termed intermediate impact velocities, which cause

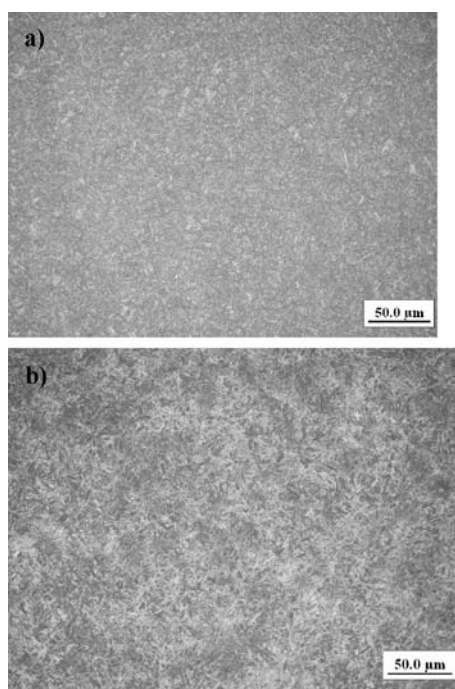


Figure 2: Microstructures of the sample AISI 4140 with a hardness of a) 40 HRC, b) 60 HRC before testing

Slika 2: Mikrostruktura vzorca AISI 4140 s trdotama a) 40 HRC in b) 60 HRC pred preizkusom

quasi-static and dynamic damage to the target material²⁵. Therefore, the projectile generates compressive shock waves on impact. These waves induce phase transformations and chemical changes, which can harden metals to a great extent²⁵.

After the ballistic testing of the steel samples, some microstructural changes were recorded. These changes were mainly the formation of ASBs. A general view of a typical ASB in the investigated samples is seen in **Figure 3**. One can see that the ASBs were formed in all samples under the effect of AP projectile and appear as long

white strips. However, the density of the ASBs varied significantly with respect to the hardness and thickness of the samples. The microstructure of the deformed ASBs in the specimen group A was very similar to that of the matrix material. In addition, the extent of the ASB formation was fairly low in comparison to the other groups B and C. Furthermore, only deformed bands were observed in the samples of group A and distortion in the bands was rather low. On the other hand, in the specimen groups B and C, both deformed and transformed bands were found. Moreover, a higher distortion in the deformed bands induced by shear in these specimen groups was seen significantly in comparison to the samples of group A. In our previous study¹⁴, the transformed band formation was also found for the steel samples (AISI 4340 and DIN 100Cr6) with the hardness of 49 HRC and 59 HRC even though the most of the bands were of the deformed type in all the samples.

The thickness of the bands seen in the investigated samples is given in **Table 1**. It changed between 19 µm and 56 µm, depending on the types of band and the sample. This indicates that the local deformation and heating in the samples is taking place. **Figure 4** represents the deformed band formed in the sample A2. It is clear that the microstructure of the band was the same with the base tempered martensitic structure. However, the color of the martensite laths in the deformed band was remarkably different from that of the matrix microstructure. This was probably due to the shear action causing a different orientation of the martensite laths in the band with respect to the base microstructure. **Figure 5** illustrates the band formation in the sample B5. It is apparent that both deformed and transformed bands appeared in this sample. The transformed bands formed as white lines and their microstructures were invisible with an optical microscopy analysis as opposed to deformed bands. A similar situation was also found in the sample group C (**Figure 6**). The thinning and

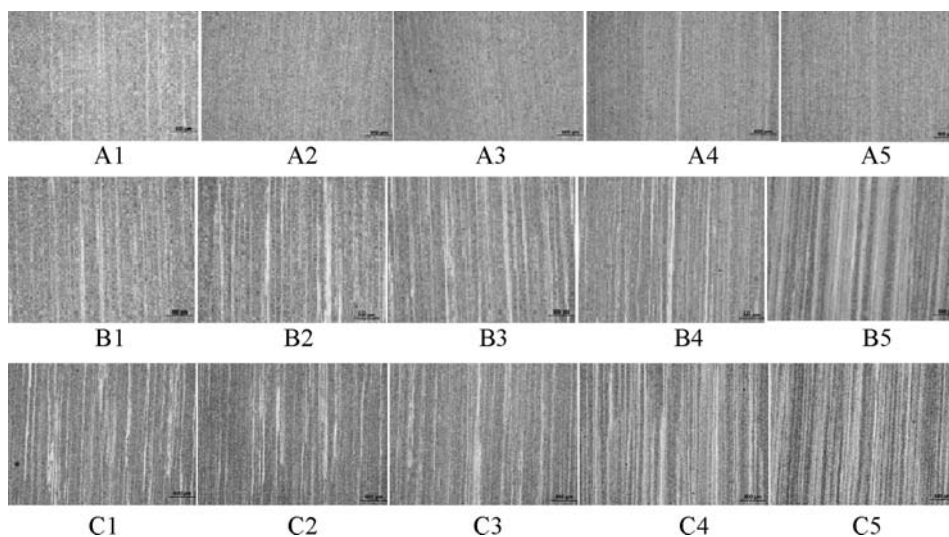


Figure 3: General view of ASBs in samples with various hardness and thickness

Slika 3: Splošen videz ASB v vzorcih z različno trdoto in debelino

Table 1: Shear band widths of the samples

Tabela 1: Širina pasov v vzorcih

Sample ID	Average Band Width (µm)	Band Type
A1	27	Deformed
A2	28	
A3	36	
A4	25	
A5	42	
B1	56	Deformed
B2	49	
B3	34	
B4	51	
B5	49	
B1	21	Transformed
B2	24	
B3	25	
B4	32	
B5	36	
C1	35	Deformed
C2	41	
C3	25	
C4	54	
C5	40	
C1	19	Transformed
C2	32	
C3	25	
C4	25	
C5	35	

shortening of the martensite laths in a transformed band of C5 can be clearly seen in **Figure 6b**. Furthermore, white areas of this band were resolved by SEM analysis. **Figure 7** depicts the detailed microstructure features for this transformed band in the sample C5 steel after the ballistic impact. In white regions of the band, fine

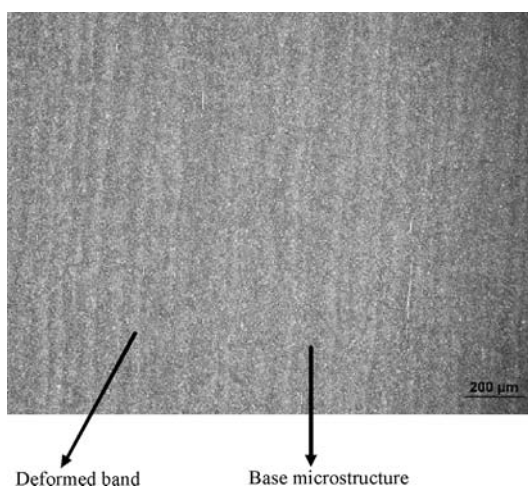


Figure 4: Microstructure of the sample A2 after ballistic testing. Deformed band formation with a lighter color compared to the base microstructure (tempered martensite) was observed.

Slika 4: Mikrostruktura vzorca A2 po balističnem preizkusu. Opaženo je formiranje deformacijskih pasov s svetlejšo barvo v primerjavi z osnovno mikrostrukturo (popuščeni martenziti)

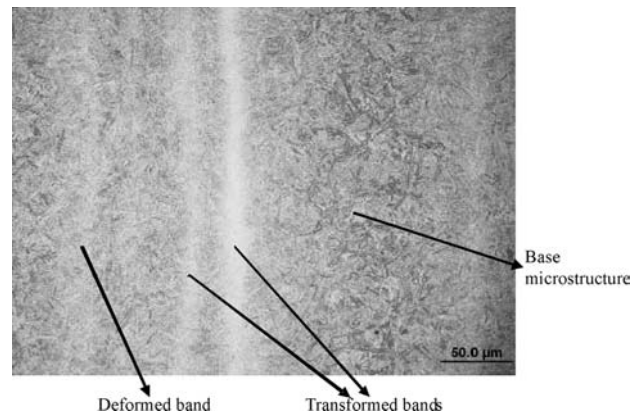


Figure 5: View of deformed and transformed bands in the sample B5 after ballistic testing. Transformed band was observed as a white line.

Slika 5: Videz deformiranih in premenjenih pasov v vzorcu B5 po balističnem preizkusu. Premenjeni pas je viden kot bela črta

iron-carbide precipitates, consisting of a small amount of chromium, were observed (**Figure 7**). The size of precipitates changed between ≈ 100 nm and $5 \mu\text{m}$. In addition, fine grains were also observed in the band. **Figure 8** shows the elemental analysis for the fine precipitate found in this band by EDX analysis. The formation of very fine grains and precipitates and very fine ferrite grains can be explained by the dynamic recrystallization. The impact velocity and kinetic energy of the projectile were sufficient to generate an immediate local heating through very narrow bands in the investigated steel AISI 4140. A ballistic study on the 30CrMnMo steel ¹⁰ also showed the formation of different types of shear bands. The fine-grain and

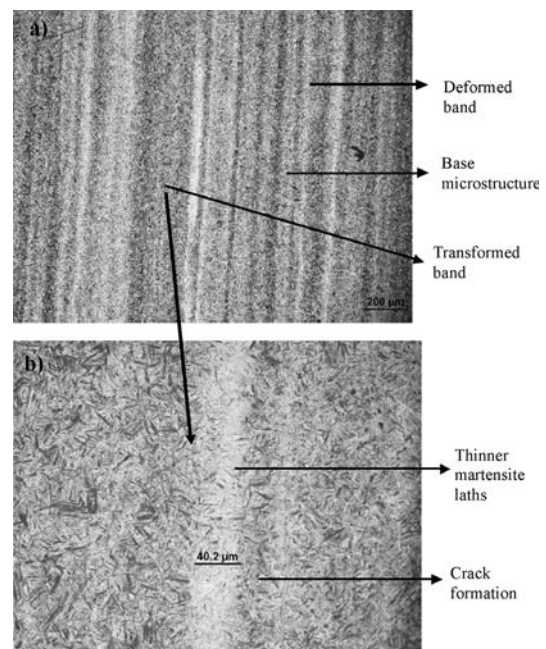


Figure 6: View of the band formation in the sample C5 after the impact of the 7.62-mm AP projectile. a) 100-times, b) 500-times.

Slika 6: Formiranje pasov v vzorcu C5 po trku AP-kroglice 7,62 mm: povečave: a) 100-kratna, b) 500-kratna

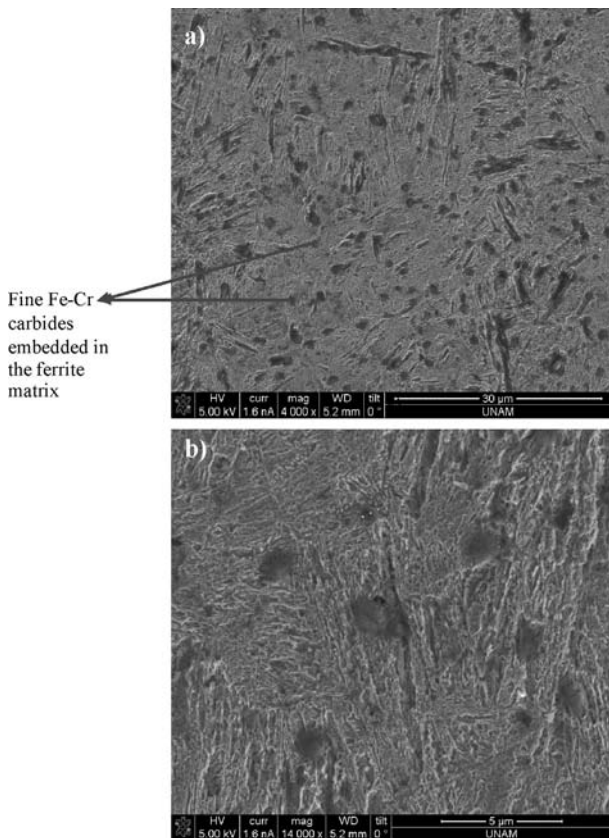


Figure 7: SEM examination of a transformed band formed in the sample C5. Formation of fine precipitate and grain occurred. a) 4000X, b) 14000X.

Slika 7: SEM-posnetki premenjenega pasu v vzorcu C5. Nastala so majhna zrna in izločki. Povečave: a) 4000-kratna, b) 14000-kratna

carbide-precipitate formations in the shear bands of the 30CrMnMo steel, observed after the impact of the tungsten-based projectile, were very similar to those found in this study.

The hardness of the bands varied with respect to the sample hardness and band type. **Table 2** gives the micro-hardness values of the bands for the investigated specimens. It is clear that the hardness of the ASBs was greater than that of the matrix for all the samples. The difference between the hardness levels of the matrix material and the ASB was smaller for the specimens of group A since the microstructural coherency and smaller

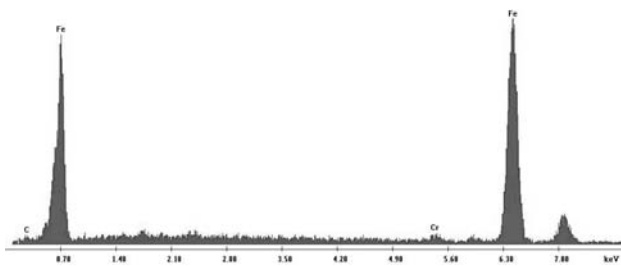


Figure 8: Elemental analysis of the fine precipitate found in the transformed band of C5 by EDX analysis.

Slika 8: Elementna EDX-analiza majhnega izločka v premenjenem pasu vzorca (c%)

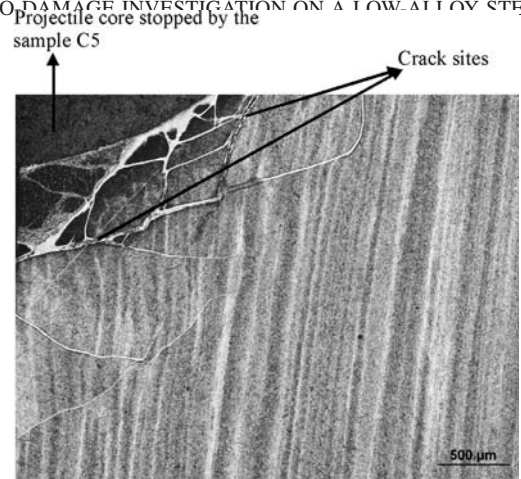


Figure 9: Micro-view of the sample C5 after the ballistic testing. The very intense ASB formation and the cracks are seen in the impact zone.

Slika 9: Mikrovidez vzorca C5 po balističnem preizkusu. V zoni udarca je nastalo veliko ASB-pasov in razpok.

Table 2: Shear bands hardness

Tabela 2: Trdota pasov

Sample Group	Types of Band	Hardness of Band (HV)	Hardness of Main Metal (HV)
A	Deformed	344	320
B	Deformed	519	417
	Transformed	569	
C	Deformed	695	667
	Transformed	722	

shear between the band and the matrix material took place. On the other hand, for the specimen groups of B and C the variation in the hardness was much higher due to the fact that the shear process occurred to a larger extent. The hardness of the deformed band (344 HV) was found to be slightly higher than that of the base material (320 HV) for the specimens of group A. However, it reached 519 HV and 695 HV for the sample groups B and C, respectively. On the other hand, the hardness of the transformed bands in the sample groups B and C was recorded as 569 HV and 722 HV, respectively. The increment in the hardness values was around 100 HV and 150 HV for the deformed and transformed bands in the sample group B, respectively. However, it was 30 HV and 50 HV for the deformed and transformed bands in the sample group C, respectively. The much higher hardness of transformed bands was directly caused by the fine structure of the grains and precipitates. A previous study²⁴ indicated that when the hardness of the AISI 4140 steel increased, the resistance to the advancement of the projectile decreased. Although the specimens belonging to the group A were perforated by a ductile hole formation mechanism under the impact of the 7.62-mm AP projectiles, most of the specimens in the groups of B and C were broken into several pieces in a brittle manner rather than perforated²⁴. In other words, the projectile perforated the samples in group A easily due their lower hardness. Furthermore, the higher resistance to projectile movement in the sample groups B

and C led to higher local heating in the steel, which accelerated the formation of the ASBs. Both the microstructure and microhardness results for the AISI 4140 steel impacted by the AP projectile were found to be similar with those of AISI 4340 and DIN 100Cr6¹⁴ due to the fact that their alloy contents are similar. All the three steels have a strong carbide-former element of chromium, which promotes the formation of carbide precipitates in the transformed ASBs during the impact. In contrast to the other two steels, the AISI 4340 steel has another alloying element of nickel, which is not a carbide forming element and so it does not affect the precipitation sequence in the formation of the transformed bands.

Borvik et al.²⁶ worked on the adiabatic shear formation in the Weldox 460E Steel impacted by blunt projectiles. They found that the target thickness heavily influenced the shear localization process. Only the deformed bands ranging from 100 µm to 300 µm in width were observed in target plates with a thickness of less than 20 mm, while the transformed bands having much less width (10–100 µm) were found for the thicker target plates²⁶. Furthermore, they measured much higher hardness values for the transformed bands (420 HV) compared to the original hardness of the steel (180–190 HV)²⁶. In a more recent study²⁷, it was recorded that the impact of the 7.62-mm AP projectile to the dual-phase steel targets caused the formation of deformed bands with higher hardness values. An increase of 70 to 100 HV in the hardness of the samples was measured after testing due to the formation of these bands²⁷. In the current study, it was also observed that an increase in the thickness of the samples caused more ASB formation. This is directly related to the increase in the resistance to projectile motion with increasing thickness. The higher portion of the kinetic energy of the projectile is transferred to the steel sample resulting in more ASB formation.

ASBs could also lead to crack formation. In other words, they can act as crack-initiation sites in the deformed materials under high strain rates. Typical crack sites occurred on the impact zone are represented for the sample C5 in **Figure 9**. Very intense ASBs led to the formation of cracks at the hit zone between the projectile and the sample. The crack formation in the sample was not detected outside the impact zone.

4 CONCLUSIONS

The main conclusions drawn from the experimental results can be described as follows:

- A deformed band formation was observed in all the steel specimens, which were tested with 7.62-mm AP projectiles. However, transformed bands occurred in the specimens having a hardness of 50 HRC or 60 HRC.
- The hardness of the bands was found to be remarkably higher than the matrix material.

- The impact action of the projectile led to the formation of fine grains and precipitates in the transformed bands.
- An increase in the resistance to the projectile motion increased the transformed band formation.
- The effect of the projectile hit on the microstructure of the AISI 4140 steel was found to be consistent with that of the AISI 4340 steel¹⁴.

Acknowledgement

This work was supported by the Research Fund of TÜBİTAK, Project # 106M211.

5 REFERENCES

- ¹ C. Zener C, J. H. Hollomon, *Journal of Applied Physics*, 15 (1944), 22
- ² R. Dornmeval, The adiabatic shear phenomenon, pp. 47–69, in *Materials at High Strain Rates*, (Ed. T. Z. Blazynski), Elsevier Applied Science, 1987
- ³ K. E. Aeberli, P. L. Pratt, *J. Mater. Sci.*, 20 (1985), 316
- ⁴ H. C. Rogers, *Ann Rev Mater. Sci.*, 9 (1979), 283
- ⁵ S. J. Manganello, K. H. Abbott, *J. Mater.*, 7 (1972), 231
- ⁶ J. L. Derep, *Acta Metall.* 35 (1987), 1245
- ⁷ C. L. Wittman, M. A. Meyers, H.R. Park, *Metall. Trans. A*, 21 (1990), 707
- ⁸ K. Cho, C. Y. Chi, J. Duffy, *Metall Trans A*, 21A (1990), 1161
- ⁹ M. N. Bassim, *J. Mater. Process. Technol.*, 119 (2001), 234
- ¹⁰ Z. Q. Duan, S. X. Li, D. W. Huang, *Fatigue Fract. Engng Mater. Struct.*, 26 (2003), 1119
- ¹¹ C-J. Hu, P-Y. Lee, J-S. Chen, *J. of the Chinese Inst. of Engineers*, 25 (2002) 1, 99
- ¹² A. G. Odeshi, M. N. Bassim, S. Al-Ameeri, *Mater. Sci. Eng. A*, 419 (2006), 69
- ¹³ J. F. C. Lins, H. R. Z. Sandim, H-J. Kestenbach, D. Raabe, K. S. Vecchio, *Mater. Sci. Eng. A*, 457 (2007), 205
- ¹⁴ M. Übeyli, T. Demir, R. O. Yıldırım, M. F. Aycan, *Kovove Materialy-Metallic Materials*, 47 (2009), 409–413
- ¹⁵ J. A. Hines, K. S. Vecchio, *ACTA Mater*, 45 (1997), 635
- ¹⁶ U. Andrade, K. Meyers, K. S. Vecchio, A. H. Chokshi, *ACTA Mater.*, 42 (1994), 3183
- ¹⁷ M. A. Meyers, U. R. Andrade, A. H. Chokshi, *Metall. Mater. Trans.*, A21 (1995), 2881
- ¹⁸ Y. B. Xu, W. L. Zhong, Y. J. Chen Q. Liu, Y. L. Bai, M. A. Meyers, *Mater. Sci. Eng.*, A 299 (2001), 287
- ¹⁹ M. A. Meyers, V. F. Nesterenko, J. C. Lasalvia, Y. B. Xu, Q. J. Xue, *Phys. IV*, 9 (2000), 51
- ²⁰ H. A. Grebe, H-R. Pak, M. A. Meyers, *Metall Trans A*, 16 (1985), 761
- ²¹ F. D. S. Marquis, Y. J. Chen, *J. Phys.*, IV C3 (1997), 441
- ²² Y. J. Chen, M. A. Meyers, V. F. Nesterenko, *Mater. Sci. Eng. A*, 268 (1999), 70
- ²³ S. Nemat-Nasser, W. Guo, *Mech. Mater.*, 32 (2000), 243
- ²⁴ T. Demir, M. Übeyli, R. O. Yildirim, *Mater. Des.*, 29 (2008), 2009
- ²⁵ D. J. Viechnicki, M. J. Slavin, M. I. Kliman, *Ceramic Bulletin*, 70 (1991), 1035
- ²⁶ T. Borvik, J. R. Leinum, J. K. Solberg, O. S. Hopperstad, M. Langseth, *Int. J. Impact Eng.*, 25 (2001), 553
- ²⁷ M. Übeyli, T. Demir, H. Deniz, R. O. Yildirim, Ö. Keleş, *Mater. Sci. Eng.*, A 527 (2010), 2036